Preparation of Nereid oligopeptide and investigation of the mechanism underlying the induction of apoptosis in human lung cancer H1299 cells

GUOMEI ZHANG*, HAN LI*, SHANSHAN LIU, MINGYANG LU, LIANG TANG and LIHUA SUN

College of Food Science and Engineering, Hangzhou Medical College, Hangzhou, Zhejiang 310013, P.R. China

Received November 8, 2021; Accepted March 18, 2022

DOI: 10.3892/mmr.2022.12710

Abstract. In the present study, oligopeptides from Nereid (*Perinereis aibuhitensis*) were prepared via enzymatic hydrolysis, and the mechanism underlying the induction of apoptosis in H1299 cells was investigated. According to the analysis of the inhibition rate on proliferation, alkaline protease demonstrated the best enzymatic efficiency. The optimal conditions for hydrolysis were as follows: 50˚C and pH 10 for 6 h; a material-to-liquid ratio of 1:1 (g/ml); and addition of 400 U/g enzyme. The hydrolysates were purified using ultrafiltration, anion chromatography, gel filtration chromatography, and high-performance liquid chromatography. The Nereid oligopeptide (NOP), with a molecular weight of 841 kDa and an amino acid sequence of glutamine-isoleucine-asparagine-glutamine-histidine-leucine, was obtained. NOP inhibited the proliferation of H1299 cells in a time- and dose-dependent manner. Morphological changes and apoptosis were also induced by NOP in H1299 cells. The western blot analysis revealed that the B-cell lymphoma 2/Bcl-2 associated X (Bcl-2/Bax) ratio was reduced by 24.7% in the NOP treatment group compared with the control group. The relative expression levels of cleaved caspase-9 (cleaved-CASP9) and cleaved caspase-3 (cleaved-CASP3) in the NOP treatment group were 2.55- and 1.71-fold higher than those measured in the control group, respectively. These results suggested that NOP exerts antitumor effects by influencing the proliferation and apoptosis of H1299 cells.

Correspondence to: Professor Lihua Sun, College of Food Science and Engineering, Hangzhou Medical College, 182 Tianmushan Road, Hangzhou, Zhejiang 310013, P.R. China
E-mail: sunlihua_002@163.com

*Contributed equally

Abbreviations: NOP, Nereid oligopeptide; CASP3, caspase-3; CASP9, caspase-9; IR, inhibition rate

Key words: Perinereis aibuhitensis Grube, oligopeptides, antitumor, H1299 cells, apoptosis

Introduction

Lung cancer is one of the most common malignancies worldwide, and associated with high rates of morbidity and mortality (IARC, 2020). There are few early symptoms, and their onset is relatively insidious. Therefore, most cases are confirmed at mid and late stages of lung cancer. Currently, chemotherapy and surgery are the most commonly used treatment modalities, which can increase the survival rate of patients. However, long-term chemotherapy also severely impacts important organs and induces drug resistance in tumors (1). The marine environment, characterized by high salt content, high pressure, and low temperature, markedly differs from the terrestrial environment. Numerous marine organisms can produce massive active substances with novel structures that differ from those synthesized by terrestrial organisms. Recent research on marine drugs has found that numerous bioactive substances of marine origin can significantly inhibit tumor growth in various ways (2,3). Therefore, there is increasing interest in discovering new anticancer drugs with low toxicity and high efficacy from marine organisms. It is expected that a diverse array of active substances of marine origin, such as peptides, polysaccharides, alkaloids, terpenes, and macrolides, will be developed into new antitumor drugs (4). For example, dolastatin-10 (obtained from the sea hare) has been used in clinical trials (5).

Nereids are invertebrates of the polychaete family (Nereidae). They are widely distributed in the Sea of Japan and the Pacific coast, and endemic to Japan and China. In recent years, the interest in the bioactive substances produced by the Nereids has gradually increased. Japanese scholars have isolated biologically active polypeptides from the Nereids (6). These polypeptides can strongly shrink the esophagus of annelids. The first isolation and purification of a protease from the Nereids were achieved at Bethune School of Medicine, Jilin University (Jilin, China). This protease is a serine protease with a molecular weight of 29 kDa, an isoelectric point of 4.4, and an optimal temperature of 60˚C. The protease exerts a strong effect on the degradation of fibrin and fibrinogen. The order of hydrolysis is as follows: Aα, Bβ, and γ chains. Studies suggested that the protease isolated from the Nereids can significantly inhibit various leukemic cells *in vitro* (7). The protease *Nereis virens* proteinase (ASP) also has strong antitumor activity in leukemic cells and lung cancer

SPC-A-1 cells (8-12). However, there is limited knowledge on the enzymatic hydrolysis of Nereid oligopeptides (NOP), and their inhibitory effects on non-small cell lung cancer H1299 cells. The objective of the present study was to investigate the preparation of an NOP and its effects on the growth of H1299 cells. Moreover, the induction of cell apoptosis and the mechanism of action are preliminarily discussed, thereby providing an experimental basis for the clinical application of NOP.

Materials and methods

Samples and reagents. The Nereid was purchased from Zhoushan Jusha Aquaculture Co., Ltd., and was identified as *Perinereis aibuhitensis* Grube by Professor Zhao Shenglong from Zhejiang Ocean University (Zhoushan, China). Trypsin, papain, alkaline protease, neutral protease, and pepsin were purchased from YTHX Biotechnology Co., Ltd. Fetal bovine serum was obtained from Hangzhou Sijiqing Biological Engineering Co., Ltd. RPMI-1640 powder and medium were purchased from Gibco; Thermo Fisher Scientific, Inc. Methyl thiazolyl tetrazolium (MTT) and dimethyl sulfoxide were purchased from Sigma-Aldrich; Merck KGaA. The other reagents were of analytical grade.

Cells and cell culture. Human lung cancer cell lines [A549 (cat. no. SCSP-503), H1299 (cat. no. SCSP-589) and 95C (cat. no. SNL-168)] and neuroblastoma [PC-12 (cat. no. SCSP-517) and SK-N-SH (cat. no. SCSP-5029)] cell lines were purchased from the Shanghai Cell Bank of the Chinese Academy of Sciences. The cells were passaged and subcultured in RPMI-1640 nutrient solution containing 10% bovine serum. All cells were static and incubated at 37˚C in a humidified atmosphere with 5% CO_2 (Forma™ cat. no. 3111; Thermo Fisher Scientific, Inc.); the culture medium was changed once every 2-3 days.

Equipment and instruments. The equipment and instruments included the following: refrigerated centrifuge (NUAIRE), carbon dioxide incubator and microplate reader (both from Thermo Fisher Scientific, Inc.), protein electrophoresis and western blotting system (Bio-Rad Laboratories, Inc.), Odyssey Imager (LI-COR Biosciences), horizontal shaker (Hangzhou Miu Instruments Co., Ltd.), clean bench (Suzhou Cleaning Equipment Co., Ltd.), -80˚C ultra-low temperature incubator (Haier Group), ice machine (Changshu Xueke Electric Co., Ltd.), and electric-heated thermostatic water bath (Changzhou Guohua Electric Appliance Co., Ltd.).

Preparation of Nereid enzymatic hydrolysates and NOP separation and purification

Selection of enzyme species. The Nereid was rinsed and homogenized. Homogenized samples (13,14) (10.0 g each) were obtained for enzymatic hydrolysis with five enzymes (i.e., trypsin, alkaline protease, neutral protease, pepsin, and papain) at certain temperatures and pH values (Table I). The optimal conditions for hydrolysis were as follows: 50˚C and pH 10 for 6 h, a material-to-liquid ratio of 1:1 (g/ml), and addition of 400 U/g enzyme. Following hydrolysis, the samples were inactivated in a water bath at 100˚C for 10 min, and centrifuged at 10,000 x g, at 4˚C for 20 min in the refrigerated centrifuge. The supernatant was obtained and examined using the MTT method to determine the inhibition rate (IR) on the proliferation of H1299 cells. This process permitted the recognition of the optimal enzyme species.

Optimization of enzymatic hydrolysis conditions. The optimal protease was used for enzymatic hydrolysis to determine the optimal temperature and pH. The relevant literature detailing single factor experiments (15-17) involving temperature, pH, material-to-liquid ratio, duration, and the amount of enzyme added during the enzymatic hydrolysis, were reviewed. Subsequently, an orthogonal test (Table II) involving the aforementioned parameters was designed, using the IR as an indicator to determine the optimal conditions for enzymatic hydrolysis.

NOP separation using ultrafiltration. Enzymatic hydrolysate <3 kDa was separated using the membrane ultrafiltration technique, cooled down, and dried. The MTT method was used to detect the IR in A549, H1299 and 95C cells after 24 h of intervention with different components at 4,000 mg/l. Next, the cell lines demonstrating more pronounced anti-lung cancer effects after treatment were identified for further separation.

NOP separation through diethylaminoethanol (DEAE) Sepharose Fast Flow chromatography. The ultra-filtrated components at 0.25 g/ml were further separated using DEAE Sepharose Fast Flow (Beijing Asia-Pacific Hengxin Biological Technology Co., Ltd.) chromatography. Following centrifugation (10,000 x g, 4˚C, 20 min), the supernatant was collected, filtered with a filter membrane (pore size, 0.22 μm), and eluted. The separation conditions were as follows: Column size, 3.6x20 cm; packing material, DEAE Sepharose FF; column particle diameter, 45-165 μm; sample volume, 2 ml; eluent, 0-0.4 mol/l NaCl solution; gradient elution, ~50 ml for each column; flow rate, 1 ml/min; detection wavelength, 280 nm; and collected volume, 5 ml per tube. The peaks were collected, concentrated, and freeze-dried. The MTT method was applied to select the peak components with the highest IR (inhibition rate) for further separation.

NOP separation using Sephadex G-25. The components with the highest IR collected in the previous step were further separated and purified by chromatography using the Sephadex G-25 column (Beijing Asia-Pacific Hengxin Biological Technology Co., Ltd.). The mass concentration of the sample was 0.25 g/ml. Following centrifugation (10,000 x g, 4˚C, 20 min), the supernatant was filtered with a filter membrane (pore size, 0.22 μm) and eluted. The conditions for separation were as follows: Column size, 2.6x60 cm; packing material, Sephadex G-25; column particle diameter, 50-150 μm; sample volume, 2 ml; eluent, distilled water; flow rate, 1.0 ml/min; detection wavelength, 280 nm; and collected volume, 5 ml per tube. The peaks were collected, concentrated, and freeze-dried. The MTT method was used to identify the peak components with the highest IR (inhibition rate) for further separation.

Separation and purification using high-performance liquid chromatography (HPLC). The peak components with the highest IR in H1299 cells collected in the previous step were further separated and purified. The chromatographic

Table I. Optimal temperature and pH value for enzymatic hydrolysis.

Enzyme	Temperature (˚C)	pH value
Trypsin	50	8.0
Alkaline protease	45	10.0
Neutral protease	45	7.0
Pepsin	37	3.0
Papain	45	6.0

Table II. Orthogonal test design.

	Factor				
Level	A	B	C	D	E
1	35	7	1:1	2	400
2	40	8	1:2	4	600
3	45	9	1:3	6	800
4	50	10	1:4	8	1,000

A, temperature, ˚C; B, pH value; C, material-to-liquid ratio, g/ml; D, time, h; E, amount of enzyme added, U/g.

conditions were as follows: Chromatographic column, Luna 10u C18(2) analytical column (10x250 mm; 5 μm); detection wavelength, 280 nm; flow rate, 1.0 ml/min; mobile phase A, acetonitrile; mobile phase B, ultrapure water (containing 0.05% trifluoroacetic acid); gradient elution, 20-100% elution A for 5-20 min; column temperature, 25˚C; and automatic sampling with a sample volume of 100 μl. The most active components were collected, freeze-dried, and sequenced as described below.

Determination of molecular weight and N-terminal sequencing of target peptides. The collected components with the highest activity were freeze-dried for the measurement of the relative molecular weight and N-terminal sequencing of target peptides at APTBIO.

MTT assay for the detection of the anti-proliferative activity of NOP. H1299 cells were seeded into 96-well culture plates (density, $1x10^5$ cells/ml) and cultured in RPMI-1640 medium (200 μl per well) under conventional conditions. After 24 h, the culture medium was removed, and a blank control (no drug treatment, RPMI-1640 medium used) group and a drug group were prepared. The cells in the drug group were treated with NOP (250, 500, or 1,000 mg/l) for 12 and 24 h at 37˚C in a humidified atmosphere with 5% CO_2. Subsequently, the culture solution was discarded, and phosphate-buffered saline (PBS) containing 10% MTT reagent was added. The cell culture was continued for 4 h. The solution was removed again, dimethyl sulfoxide (150 μl) was added, and the cells were thoroughly mixed. The cell absorbance at 490 nm was detected using a microplate reader. The cell proliferation IR (%) was calculated using the following equation: IR (%)=[1-(A treated/A control)] x100%.

Cell Counting Kit-8 (CCK-8) assay for the detection of the anti-proliferative activity of NOP. Cell culture and drug administration were designed as above. CCK-8 reagent (Shanghai Biyuntian Biotechnology Co., Ltd.) (10 μl) was added, and the cell culture was continued for 4 h. The cell absorbance at 450 nm was detected using a microplate reader. The IC_{50} which is a measure of the potency of a substance when the half maximal inhibitory concentration is achieved was calculated as follows: $IC_{50}=lg^{-1}[Xm-i(\Sigma P-0.5)]$.

Observation of cell morphology using hematoxylin and eosin (H&E) staining. Acid-treated coverslips were placed onto 96-well plates, and A549 cells were routinely cultured (density, $1x10^5$ cells/ml) for 24 h. The culture medium was subsequently removed, and a blank control group and a drug group were prepared. The cells in the drug group were treated with NOP (250, 500, or 1,000 mg/l). After 24 h of culture, the coverslips were removed, and the cells were fixed in 95% ethanol for 20 min at room temperature. The samples were stained using hematoxylin for 3-5 min at room temperature, immersed in tap water, developed with eosin for 1 min, dehydrated with ethanol, treated with xylene to become transparent, mounted in neutral gum, and images were captured under an optical microscope (BX2-FLB3 fluorescence microscope; Olympus Corporation).

Morphology of tumor cells after treatment with NOP using a transmission electron microscope. H1299 cells ($1x10^7$ cells/ml) cultured for 24 h were digested and transferred to a 10-ml centrifuge tube. This was followed by centrifugation at 800 x g at 4˚C for 6 min, washing with PBS (800 x g, 4˚C for 6 min), and removal of the supernatant. Subsequently, 2.5% dialdehyde was added, and the cell suspension was incubated overnight at 4˚C. The cell suspension was treated at the Biological Laboratory of Zhejiang University Medical College (Hangzhou, China). The cells were fixed using 2.5% glutaraldehyde at 4˚C for 24 h. Sections were cut to a thickness of 100 nm and uranyl acetate and lead citrate were used to stain cells at room temperature for 15 min. The cells were embedded in resin at 37˚C for 4-6 h, and 60˚C for 40 min. Finally, it was observed and images were captured under a transmission electron microscope.

Cell apoptosis analysis. Apoptotic rates were measured by flow cytometry using Annexin V-fluorescein isothiocyanate/propidium iodide (FITC/PI) staining. H1299 cells ($1x10^6$ cells/ml) were firstly seeded in six-well flat-bottomed plates and incubated for 24 h at 37˚C. Cells were subsequently treated with NOP (250, 500, or 1,000 mg/l) for another 24 h at 37˚C and harvested. After digestion with trypsin, the cells were suspended in PBS and harvested by centrifugation at 800 x g at room temperature for 10 min. Next, the cells were incubated with Annexin V-FITC (5 μl) and PI (10 μl) at room temperature for 15 min in the dark. After staining, cells were immediately analyzed using flow cytometry (Easy Cyte6 HT-2L Flow Cytometer; Luminex Corporation).

Western blot analysis. Total protein was extracted with radioimmunoprecipitation assay (RIPA) lysis buffer (Beijing Solarbio Science & Technology Co., Ltd.), and protein concentrations were determined using a bicinchoninic acid assay kit. Proteins

Table III. Orthogonal experiment design and results.

Number	A	B	C	D	E	IR (%)
1	1 (35)	1 (7)	1 (1:1)	1 (2)	1 (400)	90.34±1.23
2	1	2 (8)	2 (1:2)	2 (4)	2 (600)	40.11±1.45
3	1	3 (9)	3 (1:3)	3 (6)	3 (800)	51.43±0.88
4	1	4 (10)	4 (1:4)	4 (8)	4 (1,000)	38.78±2.45
5	2 (40)	1	2	3	4	56.41±3.02
6	2	2	1	4	3	58.47±2.41
7	2	3	4	1	2	42.12±0.88
8	2	4	3	2	1	88.71±1.69
9	3 (45)	1	3	4	2	41.58±2.45
10	3	2	4	3	1	42.01±3.21
11	3	3	1	2	3	41.89±1.12
12	3	4	2	1	4	43.25±2.47
13	4 (50)	1	4	2	3	49.64±0.89
14	4	2	3	1	4	54.11±2.11
15	4	3	2	4	1	55.54±2.55
16	4	4	1	3	2	89.32±1.76
K1	55.165	59.492	70.005	57.455	69.150	
K2	61.427	48.675	48.827	55.087	53.282	
K3	42.183	47.745	58.957	59.792	50.698	
K4	62.152	65.015	43.138	48.592	47.797	
R	19.969	17.270	26.867	11.200	21.353	

A, temperature, ˚C; B, pH value; C, material-to-liquid ratio, g/ml; D, time, h; E, amount of enzyme added, U/g; IR, inhibition rate.

(20 μl) were subsequently separated by sodium dodecyl sulfate-polyacrylamide gel electrophoresis and transferred to a 12 or 15% polyvinylidene difluoride membrane. The membranes were rinsed once with PBS containing 0.05% Tween-20 (PBST) and blocked in 5% skimmed milk powder at 4˚C for 2 h. After two rinses in PBST (10 ml) and one rinse in PBS (10 ml), the membranes were placed into a hybridization bag containing the primary antibodies B-cell lymphoma 2 (Bcl-2; 1:1,000; cat. no. A00040-2), Bcl-2 associated X (Bax; 1:1,000; cat. no. BA0315-2), caspase-9 (CASP9; 1:1,000; cat. no. BM4619), and caspase-3 (CASP3; 1:500; cat. no. BM4620) (all from Wuhan Boster Biological Technology, Ltd.). The antibodies were diluted with 1% bovine serum albumin solution according to the instructions provided by the manufacturer. Following incubation overnight at 4˚C, the membranes were placed on a shaker at room temperature. After 1 h, the membranes were rinsed thrice with PBST (10 min per rinse). Thereafter, the membranes were incubated with fluorescent secondary antibodies goat anti-rabbit (1:10,000; cat. no. 925-68071) and goat anti-mouse (1:10,000; cat. no. 925-68070) (both from LI-COR Biosciences) and incubated in the dark for 1 h at room temperature. Following incubation, the membranes were washed thrice with PBST (10 min per rinse). β-actin was used as an internal reference, and protein bands were quantified using the Odyssey Imager (LI-COR Biosciences).

Statistical analysis. Three parallel experiments were conducted for all groups. Experimental data were analyzed and processed using SPSS version 19.0 statistical software (IBM Corp.). One-way ANOVA with Dunnett's post hoc test was used to determine the difference between different groups. The data are expressed as the mean ± standard deviation (n=3). $P<0.05$ was considered to indicate a statistically significant difference.

Results

Optimization of the enzymolytic process of NOP. In H1299 cells, the IRs were 69.94±1.35% for alkaline protease, 62.25±2.03% for trypsin, 53.76±1.43% for pepsin, 49.62±1.09% for neutral protease, and 45.27±2.25% for papain. In addition, the order of activity was as follows: alkaline protease > trypsin > pepsin > neutral protease > papain (Fig. 1). According to the IR, alkaline protease was selected for further screening.

Orthogonal test results. The IR was determined under different enzymolysis conditions, such as temperature, pH value, material-to-liquid ratio, duration, and the amount of enzyme added (Table III). The range method was used to analyze the order of factors affecting the IR: C > E > A > B > D. The factor with the greatest impact on IR was C (material-to-liquid ratio). The optimal conditions for enzymatic hydrolysis were A4B4C1D3E1, enzymatic hydrolysis at 50˚C and pH 10 for 6 h, with a material-to-liquid ratio of 1:1 and the addition of 400 U/g enzyme.

NOP separation and purification

Ultrafiltration of NOP. After enzymatic hydrolysis, enzymatic hydrolysate <3 kDa was separated from the supernatant using

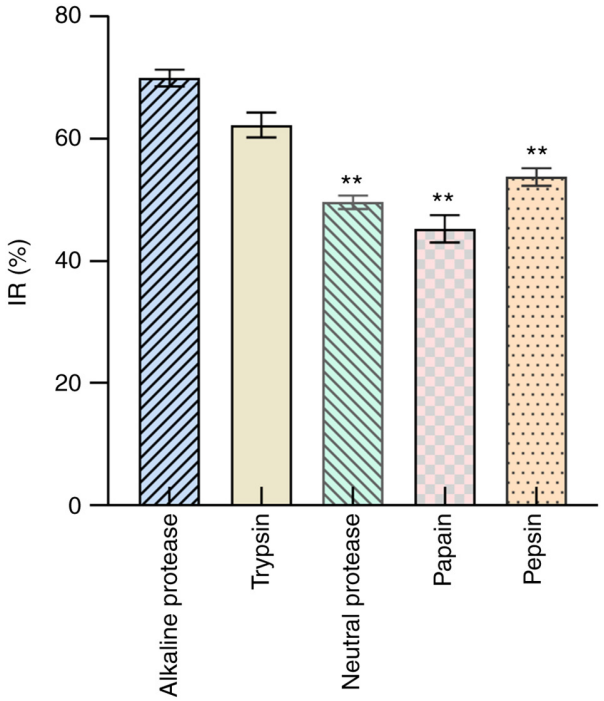

Figure 1. Inhibition rates of five types of proteolysis products for H1299 cells. IR, inhibition rate. **P<0.01 vs. alkaline protease.

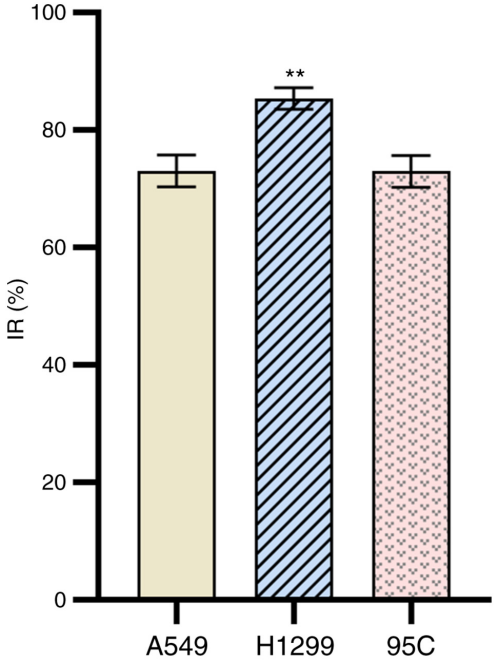

Figure 2. Inhibition rates of the enzyme hydrolysate for various lung cancer cells (A549, H1299 and 95C). IR, inhibition rate. **P<0.01 vs. A549.

an ultrafiltration membrane. The components were collected and freeze-dried, and the proliferation of various cancer cells (A549, H1299, 95C) was examined using MTT. After a 24-h intervention with the components at 2,000 mg/l, the IR of the aforementioned cells was 73.10±2.70%, 85.44±1.81%, and 73.02±2.71%, respectively (Fig. 2). These findings revealed that H1299 cells had the best IR, and could be selected for further screening.

DEAE Sepharose Fast Flow chromatography. Chromatography using a DEAE Sepharose Fast Flow column yielded two elution peaks from the enzymatic hydrolysate <3 kDa, namely NOP-1 and NOP-2 (Fig. 3A). After 24 h of intervention with these two peptides at 2,000 mg/l, the IR of H1299 cells was 36.50±3.08% and 64.47±1.25%, respectively. At a concentration of 4,000 mg/l, these values were 52.88±1.64% and 86.23±2.71%, respectively (Fig. 3B). Therefore, the second peptide was selected for further separation and purification.

Sephadex G-25 separation. The second peptide yielded in the above step was freeze-dried and separated using a Sephadex G-25 column to obtain two elution peaks, namely NOP-2-1 and NOP-2-2 (Fig. 3C). Following treatment of H1299 cells with these two peptides at a concentration of 1,000 mg/l, the IR was 53.97±3.40% and 69.33±2.27%, respectively. At a concentration of 2,000 mg/l, these values were 74.77±2.61% and 88.10±1.60%, respectively (Fig. 3D). Therefore, the second peptide with the highest activity was used for further separation and purification using HPLC.

HPLC separation. After elution and purification through HPLC, two elution peaks (NOP-2-2-1 and NOP-2-2-2) were noted (Fig. 3E). After treatment of H1299 cells with these two peptides at a concentration of 500 mg/l, the IR was 56.50±3.64% and 77.10±2.09%, respectively. At a concentration of 1,000 mg/l, these values were 70.83±1.45% and 87.97±1.89%, respectively (Fig. 3F). Thus, the second peptide with the highest activity was termed NOP. The molecular weight of the NOP was determined, and N-terminal amino acid sequencing was performed.

Molecular weight measurement and N-terminal sequencing of target peptides. The molecular weight was 841.0768 kDa, as identified by mass spectrometry at APTBIO (Fig. 4). The amino acid sequence was glutamine-isoleucine-asparagine-glutamine-histidine-leucine (Gln-Ile-Asn-Gln-His-Leu). The molecular weight of the peptide obtained by amino acid sequencing was 841.91 kDa; this finding was completely consistent with the results of molecular weight determination.

Anti-lung cancer H1299 cell activity

Proliferation of H1299 cells. After 12 h of treatment with 100 mg/l NOP, the IR of H1299 was 43.77±3.84%. At a concentration of 1,000 mg/l, this value was 76.00±2.67%. After 24 h of intervention with 100 mg/l and 1,000 mg/l NOP, this value was 58.47±2.44% and 90.07±1.56%, respectively (Fig. 5A). The 12- and 24-h IC_{50} values were 172.5 and 107.8 mg/l, respectively (Fig. 5B). Therefore, compared with control, the IR was significantly elevated in parallel with the increase in mass concentration and action time (P<0.01).

H&E staining results. H1299 cells grew well in the normal group and were tightly arranged, exhibiting good morphology. The cytoplasm was uniformly stained, the nucleus was in uniform size, and numerous nucleoli were detected (Fig. 6A). Following 24 h of treatment with NOP at low concentration (250 mg/l; Fig. 6B), the number of H1299 cells per field of view

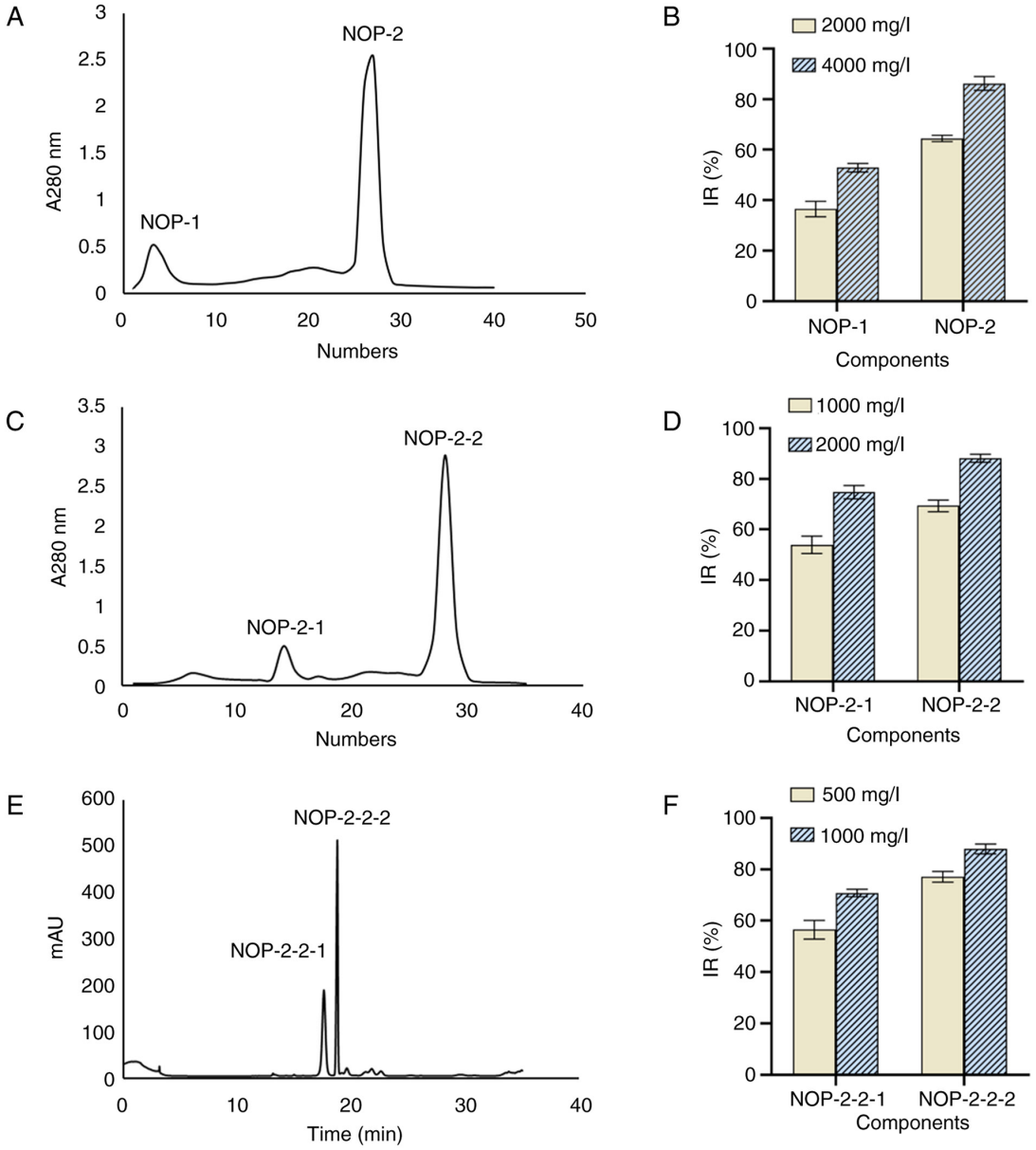

Figure 3. Isolation and purification of the NOP. (A) Enzymatic hydrolysate was separated using DEAE Sepharose Fast Flow chromatography, revealing two peaks (NOP-1 and NOP-2). (B) IR for H1299 cells treated with different concentrations of NOP-1 and NOP-2. (C) NOP-2 was separated using a Sephadex G-25 column, revealing two peaks (NOP-2-1 and NOP-2-2). (D) IR for H1299 cells treated with different concentrations of NOP-2-1 and NOP-2-1. (E) NOP-2-2 was separated through HPLC, revealing two peaks (NOP-2-2-1 and NOP-2-2-2). (F) IR for H1299 cells treated with different concentrations of NOP-2-2-1 and NOP-2-2-2. NOP, Nereid oligopeptide; DEAE, diethylaminoethanol; HPLC, high-performance liquid chromatography; IR, inhibition rate.

decreased, and numerous vacuoles appeared in the cytoplasm. The number of nucleoli decreased, and the intercellular space appeared. The cell contour was blurred, the area of plasma membrane was enlarged, the cytoplasm was vacuolated, the nucleus appeared nuclear pyknosis and the number of nucleoli was reduced (500 mg/l; Fig. 6C), After 24 h of treatment with NOP at a high concentration (1,000 mg/l; Fig. 6D), the cell contour was blurred, with irregular shape and numerous protrusions. Morphological changes, such as chromatin condensation and pyknosis, were also observed (Fig. 6D).

Cell ultrastructural changes. Under the transmission electron microscope, H1299 cells in the control group showed dense microvilli on the surface and had rich cytoplasm without swelling. Moreover, the mitochondria were relatively intact, there were no obvious effects on the endoplasmic reticulum, and the plasma and nuclear membranes were relatively intact (Fig. 7A and B). After intervention with 1,000 mg/l NOP, the cells were almost round in shape without microvilli, but with obvious cytoplasmic swelling. In addition, the cell membrane was disrupted, swelling of the nuclear membrane was observed, the endoplasmic reticulum was severely vacuolated, and a large number of vacuoles appeared in the cytoplasm (Fig. 7C). After treatment with NOP at a high concentration (1,000 mg/l; Fig. 7D), H1299 cells had broken plasma and nuclear membranes, a shrunken nucleus, heterochromatin aggregation, extended smooth endoplasmic reticulum, and swollen mitochondria. More obvious changes were observed as the concentration of NOP increased. Under the transmission electron

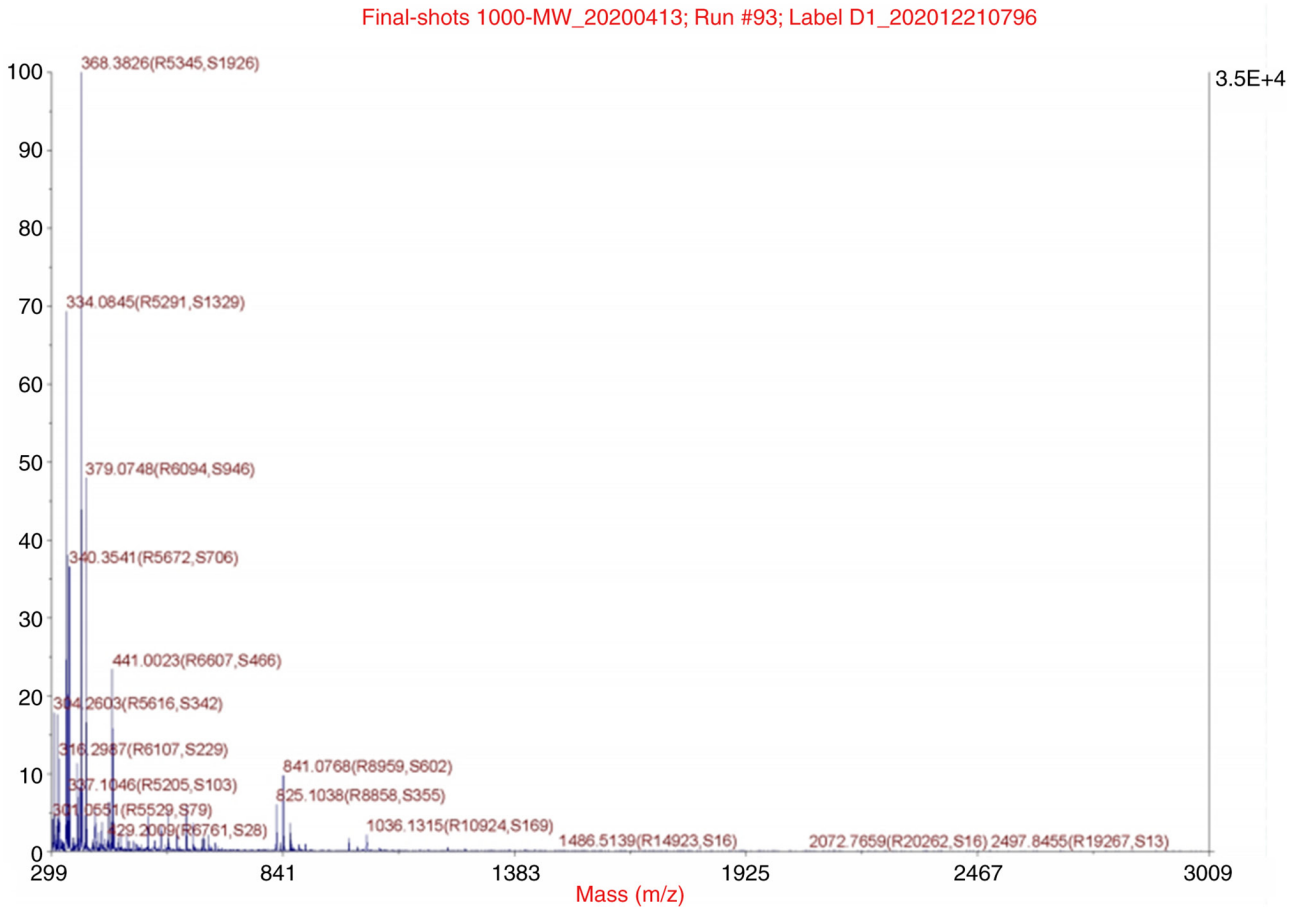

Figure 4. Molecular weight of the target peptide (FW: 841.0768).

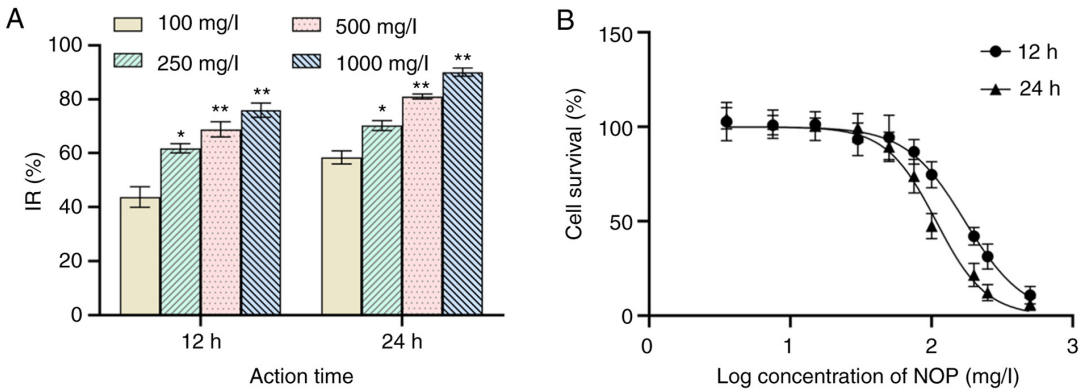

Figure 5. Effect of NOP on the proliferation of H1299 cells. (A) Inhibition rates of the NOP for H1299 cells at different time-points and under different concentrations. (B) Survival of H1299 cells after treatment with the NOP at different time-points and under different concentrations. *P<0.05 and **P<0.01 vs. the 100 mg/l. NOP, Nereid oligopeptide; IR, inhibition rate.

microscope, H1299 cells exhibited apoptotic characteristics after 24 h of exposure to NOP.

Detection of the apoptotic rate of cells by flow cytometry. In order to quantitatively measure the NOP-induced apoptosis in H1299 cells, Annexin V-FITC and PI double staining was used to determine the number of apoptotic cells. As revealed in Fig. 8, for the control, the percentage of Annexin V-FITC-stained H1299 cells was 7.08±0.65%. After 24 h of exposure to 250, 500, and 1,000 mg/l NOP, the percentage of apoptotic cells increased to 11.93±0.75%, 12.52±1.16%, and 24.36±1.53%, respectively (Fig. 8). The apoptotic effect on H1299 cells was significantly enhanced with the increasing concentration of NOP compared with that observed in the control group. Therefore, NOP was able to effectively induce apoptosis in H1299 cells.

Western blotting. The protein bands of Bcl-2, Bax, cleaved-CASP9, and cleaved-CASP3 in samples obtained from H1299 cells treated with different concentrations of NOP for

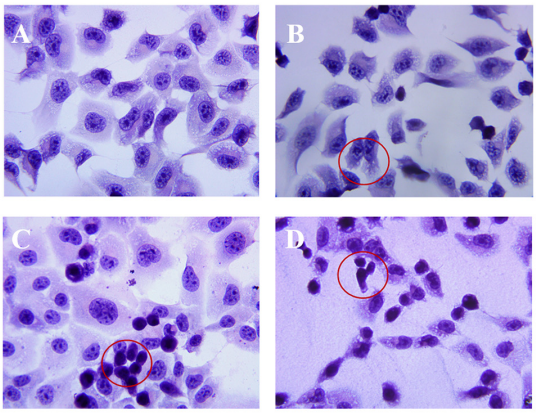

Figure 6. H&E staining images of H1299 cells after treatment with NOP (x400). (A) The negative control group (normal H1299 cells) grew well, had full morphology, clear borders, and a large number of nucleoli. (B) Treatment of H1299 cells with 250 mg/l NOP. The cell morphology was irregular, the intercellular space was enlarged, and vacuoles were detected in the cytoplasm (red circles). (C) Treatment of H1299 cells with 500 mg/l NOP. The cell morphology was irregular, the cell outline was blurred, the plasma membrane area was enlarged, vacuoles were detected in the cytoplasm, pyknosis was observed in the nucleus, and the number of nucleoli was decreased (red circles). (D) Treatment of H1299 cells with 1,000 mg/l NOP. The cell morphology was irregular, the cells shrank and became rounder and smaller, the volume was decreased, and pyknosis was observed in the nucleus (red circles). H&E, hematoxylin and eosin; NOP, Nereid oligopeptide.

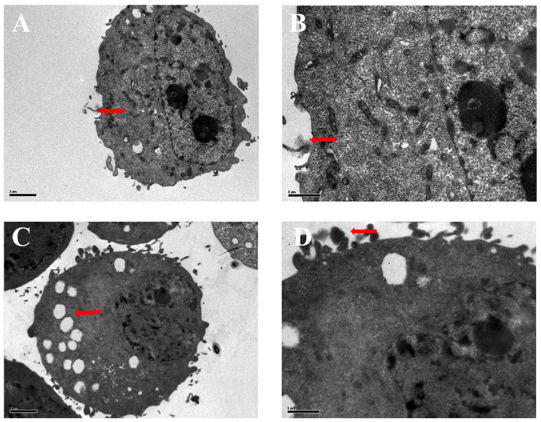

Figure 7. Ultrastructure changes in H1299 cells. (A) Magnification of the ultrastructure of normal H1299 cells (x2,500), revealing microvilli around them, less heterochromatin, and one nucleolus (red arrow). (B) Magnification of the ultrastructure of normal H1299 cells (x5,900), demonstrating more obvious surrounding slender microvilli (red arrow). (C) Following treatment of H1299 cells with 1,000 mg/l NOP for 24 h, their ultrastructure was visualized through magnification (x2,500). The nuclear volume was reduced, the morphology was abnormal, heterochromatin edge aggregation was obvious, numerous vacuoles were detected in the cells, and the cell microvilli disappeared (red arrow). (D) Magnification of the cell ultrastructure (x5,900) after treatment with 1,000 mg/l NOP for 24 h showed an apparent increase in apoptotic bodies (red arrow). NOP, Nereid oligopeptide.

24 h are revealed in Fig. 9A. The protein expression levels of each gene are presented in Fig. 9B and C. The results showed that the levels of Bcl-2 protein were decreased, and the ratio of Bcl-2/Bax was significantly decreased in the 1,000 mg/l NOP group compared with the control group ($P<0.01$). Moreover, the levels of cleaved-CASP9 and cleaved-CASP3 were significantly upregulated, while the ratio of Bcl-2/Bax was significantly reduced by 24.72% compared with the control group. The relative expression of cleaved-CASP9 and cleaved-CASP3 was 2.55- and 1.71-fold higher than that noted in the control group, respectively. Therefore, at a certain concentration range, NOP can significantly upregulate the protein levels of cleaved-CASP9, cleaved-CASP3, and Bax, and significantly downregulate those of Bcl-2.

Activity on the proliferation of PC12 and SK-N-SH cells. Following treatment of PC12 and SK-N-SH cells with 250 mg/l NOP for 24 h, the IR was 106.52±0.92% and 102.53±1.24%, respectively. At a concentration of 1,000 mg/l, these values were 119.38±1.10% and 110.41±0.52%, respectively (Fig. 10). Higher mass concentration indicated higher IR. The differences between the control and NOP groups were statistically significant ($P<0.05$). These findings indicate that NOP did not exert a toxic effect on PC12 and SK-N-SH cells; in contrast, it promoted cell proliferation.

Discussion

Bioactive peptides are composed of multiple amino acids linked by peptide bonds (18). They exert several beneficial effects on the human body (e.g., anti-swelling, analgesic, immune-modulatory, anti-viral, and anti-hypertensive). Currently, there are three main methods utilized for the extraction of bioactive peptides, namely direct extraction, synthesis, and hydrolysis. The direct extraction method is only suitable for laboratory extraction of some natural bioactive peptides with low content and complex structure in animals and plants. Although it is easy to obtain pure bioactive peptides using the synthetic method, its large-scale use is limited by the high cost and numerous adverse reactions. Hydrolysis can be divided into two types, namely chemical and enzymatic. The latter is a controllable process, in which the proteins are hydrolyzed using appropriate proteases (19,20). It is characterized by mild conditions, a controllable process, high yield, and good safety. Enzymatic hydrolysis has been used to extract peptides from marine organisms, which have demonstrated favorable antitumor activity. For example, Zhou (21) used the compound enzymatic hydrolysis method to extract fucoidan that was deproteinized using the Sevag method. In their study, homogeneous components with reducing ability and quenching lipid peroxidation ability were obtained through chromatography using the DEAE Sepharose Fast Flow ion exchange column and Sephadex-G150 column. Zhu *et al* (22) used a two-step enzymatic hydrolysis with papain and trypsin to obtain polysaccharides from *Urechis unicinctus*, reporting a yield of 6.2%. Visceral polysaccharides from *Urechis unicinctus* are glycosaminoglycan-like, with a molecular weight of approximately $4.1x10^3$ kDa. A preliminary study investigating *in vitro* antioxidant activity revealed that visceral polysaccharides possess significant lipid peroxide scavenging activity, with a half scavenging mass concentration of 2.47 mg/ml (22). Huang *et al* (23) and Ding *et al* (24) used enzymatic hydrolysis to extract a polypeptide from cuttlefish ink. They found that this cuttlefish polypeptide could inhibit prostate cancer cells DU-145, PC-3, and LNCaP in a time- and dose-dependent manner. Therefore, in the present study, trypsin, papain, alkaline protease, neutral protease, and pepsin were used. Considering the IR as an indicator, alkaline protease was

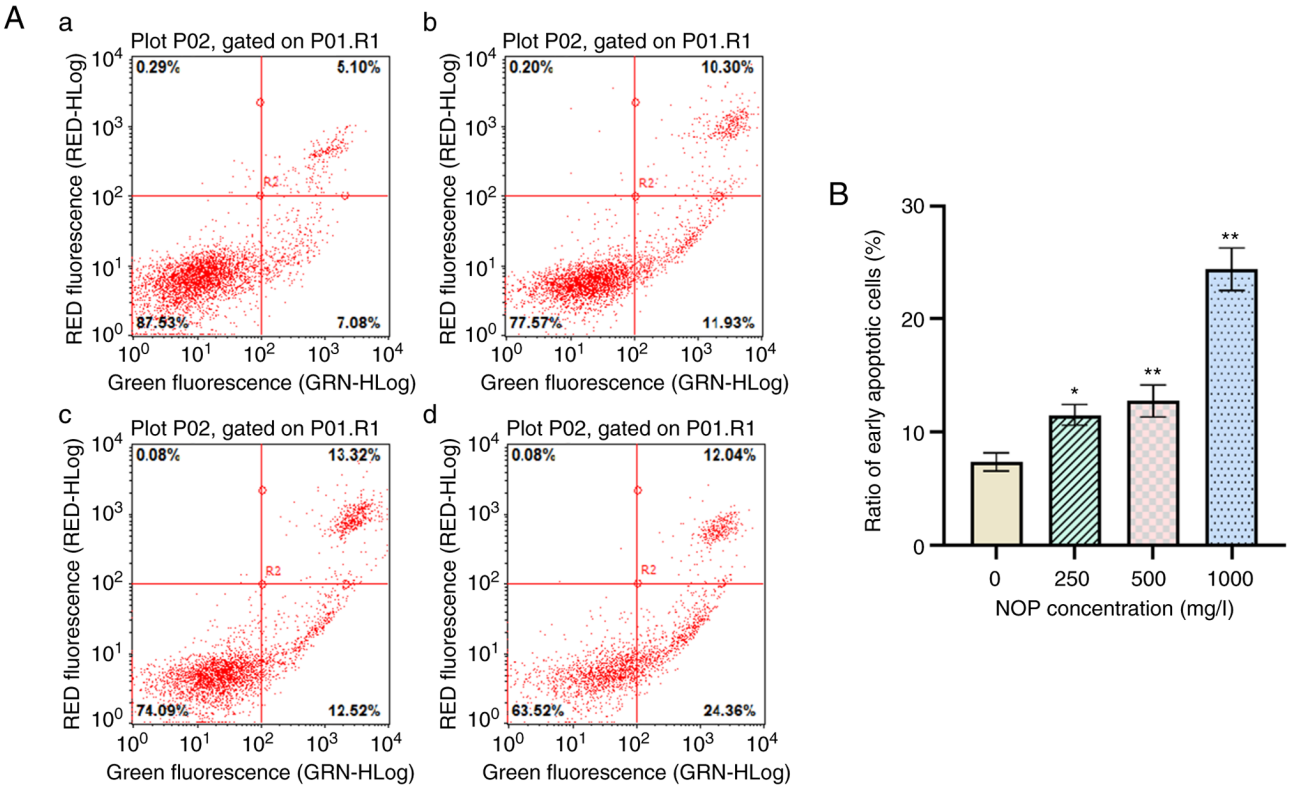

Figure 8. Apoptotic effect of NOP on H1299 cells. (A) Flow cytometric analysis of H1299 cells using double staining with Annexin V fluorescein isothiocyanate (FITC) and propidium iodide (PI). Annexin V and PI. Quadrants: lower left, live cells; upper left, necrotic cells; lower right, early apoptotic cells; upper right, late apoptotic cells. The percentage of early apoptotic cells was (a) 7.08% in the negative control cells; (b) 11.93% in the 250 mg/l NOP-treated cells; (c) 12.52% in the 500 mg/l NOP-treated cells and (d) 24.36% in the 1,000 mg/l NOP-treated cells. (B) Percentage of apoptotic cells. All data are presented as the mean ± standard deviation of measurements obtained from three experiments. *P<0.05 and **P<0.01 vs. the control. NOP, Nereid oligopeptide.

determined to be the most effective protease for NOP. According to the results of the single factor test, the enzymatic hydrolysis process was optimized through an L16 (4^5) orthogonal test. The optimal conditions for the extraction of NOP were as follows: Enzymatic hydrolysis at 50˚C and pH 10 for 6 h, a material-to-liquid ratio of 1:1, and addition of 400 U/g enzyme. The purified oligopeptide was termed NOP, and its amino acid sequence is Gln-Ile-Asn-Gln-His-Leu.

The MTT assay is a colorimetric assay for measuring cell survival and proliferation, involving the conversion of yellow-dyed MTT to bluish-purple formazan by the action of mitochondrial reductase. However, this conversion does not occur in dead cells (25). The MTT method is often used to detect inhibitory effects on cell proliferation. Ma *et al* (26) applied the MTT method to detect the proliferation of human glomerular mesangial cells treated with different concentrations of Lumbricus's active ingredients. They found that the middle dose (40 μg/ml) exerted the best effect. Using the MTT assay, Chen *et al* (27) reported that phycoerythrin had an inhibitory effect on human cervical cancer HeLa cells in a dose-effect manner. The results of flow cytometry showed that phycoerythrin arrested the cell cycle of HeLa cells from the G2/M to the S phase, thereby playing an inhibitory role. In the present study, the MTT method was used to detect the inhibitory effect of NOP on the proliferation of H1299 cells. It was determined that NOP could inhibit the activity of H1299 cells in a time- and dose-dependent manner. In other words, the IR of cells was significantly increased in parallel with the increase in the mass concentration of the NOP and time extension. The discovery of new anticancer drugs from marine organisms, including peptides, glycosaminoglycans, and macrolides, is a new goal of anticancer drug research. Marine peptides are characterized by low molecular weight, high activity, and low toxicity, and have become a research hotspot worldwide. In 1987, Pettit *et al* (28) and Cao and Song (29) isolated dolastatin-10, a small linear peptide from the sea hare. In a Phase II clinical trial, the combination of dolastatin-10 and other anticancer drugs exerted an obvious anticancer effect. Its derivatives, such as TZT-1027 (auristatin PE) and auristatin PYE, also showed significant clinical therapeutic effects (30). Chi *et al* (31) isolated two polypeptides, namely BCP-A (Trp-Pro-Pro) and BCP-B (GlnPro), from *Tegillarca granosa* Linnaeus. BCP-A exhibited a favorable effect on the IR of PC-3, DU-145, H-1299, and HeLa cells in a time- and dose-dependent manner. Following treatment with 15 mg/ml BCP-A, the early apoptotic rate of PC-3 cells increased from 11.22 to 22.78%. Yao *et al* (32) extracted a type of polypeptide from *Tegillarca granosa* Linnaeus, which induced cell cycle arrest at the G2/M and G0/G1 phases in A549 and Ketr-3 cells, respectively; these polypeptides could significantly inhibit transplanted tumors in mice. Wang *et al* (33) extracted and isolated the polypeptide Mere15 from clams through ion exchange and gel filtration. Mere15 could inhibit the growth of A549 cells in a dose- and time-dependent manner. With the increase in treatment time, cell cycle arrest at the G2/M phase was induced in A549 cells; this effect was related to

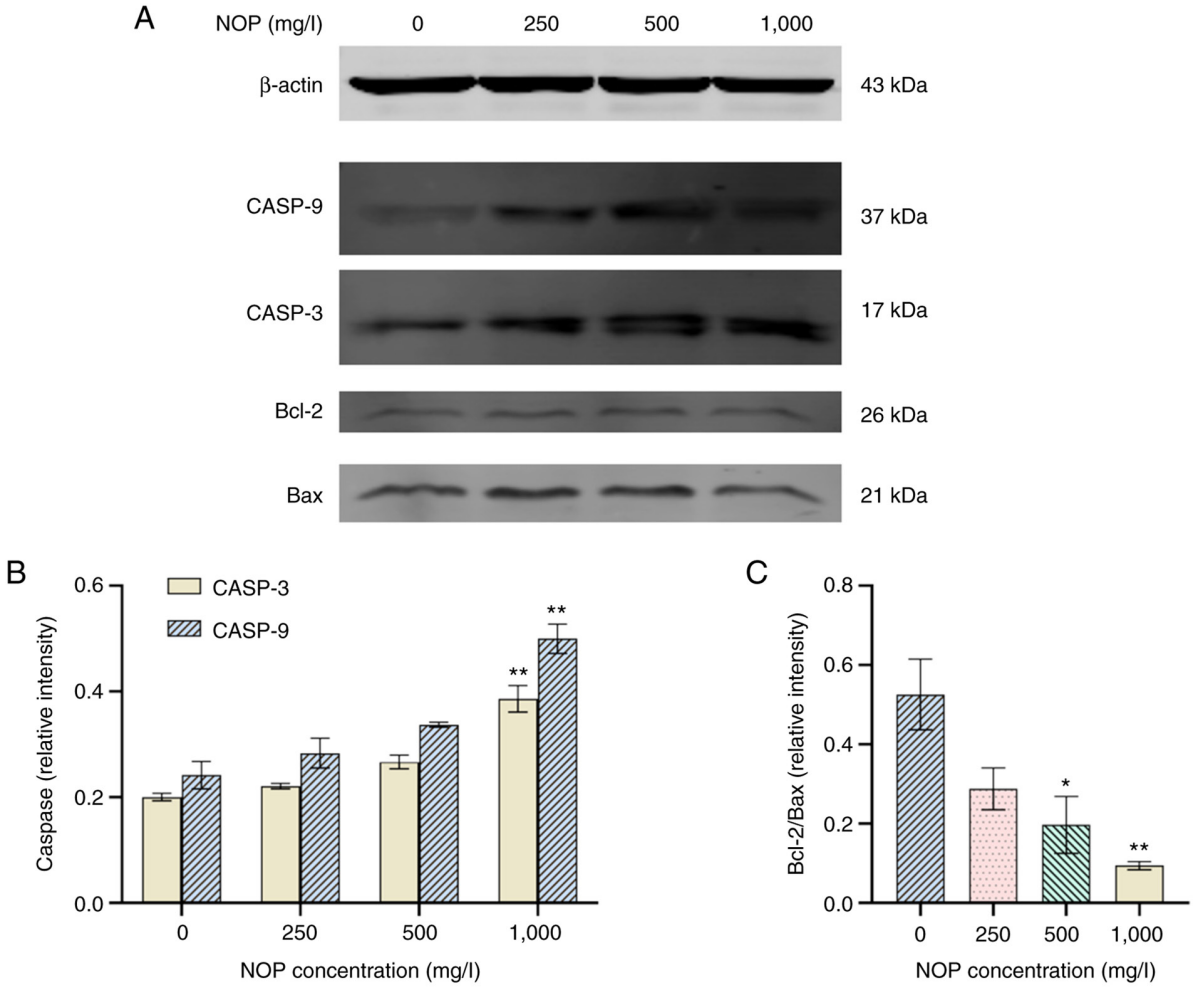

Figure 9. Western blotting. (A) H1299 cells were treated with different concentrations of Nereid oligopeptide for 24 h. The results of electrophoresis for the bands of Bcl-2, Bax, cleaved CASP9 and CASP3 proteins. (B) Expression levels of CASP9 and CASP3 proteins. (C) Changes in the ratio of Bcl-2/Bax protein expression. *P<0.05 and **P<0.01 vs. the control. Bcl-2, B-cell lymphoma 2; Bax, Bcl-2 associated X; CASP9, caspase-9; CASP3, caspase-3; NOP, Nereid oligopeptide.

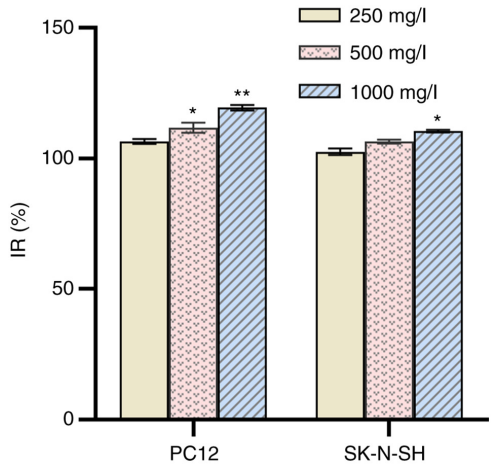

Figure 10. Inhibition rate of the Nereid oligopeptide for PC12 and SK-N-SH cells at different concentrations. *P<0.05 and **P<0.01 vs. 250 mg/l IR, inhibition rate.

the inhibition of tubulin polymerization. In the present study, the MTT method was used to detect the IR of H1299 cells treated with NOP. It was determined that H1299 cells treated with 250 mg/l NOP for 12 h exhibited apoptotic characteristics. After treatment with 1,000 mg/l NOP for 24 h, the IR of H1299 cells was increased to 90.07%.

The morphological changes strongly indicated the occurrence of apoptosis, which corresponded with a previous study (34). The characteristic morphology of early apoptotic cells could be directly detected using H&E staining under a transmission electron microscope. H1299 cells exhibited obvious cell morphological changes after intervention with NOP, such as increased intercellular space, irregular shape, decreased size, vacuoles, and apoptotic bodies in some cells. These changes became more detectable as the concentration increased. Overall, NOP extracted by alkaline protease can effectively inhibit the proliferation of H1299 cells *in vitro*. In addition, H1299 cells showed obvious apoptotic characteristics after 24 h of intervention with NOP. Thus, Annexin V-FITC was used to detect cells undergoing apoptosis, and PI was used to determine the number of necrotic cells. Flow cytometry revealed that the percentage of apoptotic cells was significantly increased in parallel with the increasing concentration of NOP. The results of the present study indicated that NOP exhibits anti-lung cancer activity through the induction of apoptosis.

Apoptosis refers to programmed cell death that is controlled by genes; it includes two classical pathways, namely the exogenous and endogenous (35,36). The endogenous apoptotic pathway is the main process of apoptosis. In the present study, the expression of related proteins, including intracellular Bax and Bcl-2, was detected using western blotting assays. The aim of this analysis was to determine whether NOP induces apoptosis in H1299 cells through the endogenous pathway. The Bcl-2 family plays a vital role in regulating the initiation of the endogenous pathway. During apoptosis, Bax and other pro-apoptotic proteins are translocated from the cytoplasm to the outer mitochondrial membrane, altering the permeability of the mitochondrial membrane. Bcl-2 and Bax regulate the release of cytochrome *c* (Cyt-C) by forming homodimers or heterodimers (37-39), and the ratio of Bcl-2/Bax is used to indicate the regulatory effect of apoptosis. Specifically, an increase in the Bcl-2/Bax ratio denotes inhibition of apoptosis. In contrast, a decrease in the Bcl-2/Bax ratio indicates promotion of apoptosis. The findings of the present study revealed that treatment with 250, 500, and 1,000 mg/l NOP significantly increased the protein expression of Bax and decreased that of Bcl-2. Moreover, the Bcl-2/Bax ratio was decreased. These effects promote the release of Cyt-C and initiate the endogenous apoptotic pathway from the upstream. Changes in the intracellular levels of activated CASP9 and CASP3 were also detected. In the mid and late stages of endogenous apoptosis, Cyt-C that enters the cytoplasm is combined with the WD repeat sequence at the carboxyl end of apoptotic protease-activating factor 1 (Apaf-1) in a 2:1 ratio to form an Apaf-1/Cyt-C complex. This complex can change the conformation of Apaf-1, inducing the formation of apoptotic bodies, triggering caspase cascade reactions, and eventually resulting in cell apoptosis (40,41). The present study showed that the protein content of activated CASP9 and CASP3 was significantly increased in parallel with the increase in the concentration of NOP. This observation indicated that activated CASP9 induces the downstream activated CASP3. CASP3 is the key executor in the downstream process of apoptosis. Activated CASP3 can degrade poly ADP-ribose polymerase, activate endonuclease, and cleave DNA strands between nucleosomes by hydrolyzation; these effects lead to DNA segmentation that is unique to apoptosis (42). The results of the present study showed that the protein levels of cleaved-CASP9 and cleaved-CASP3 were significantly increased. This indicates that NOP can activate the key downstream caspases via the endogenous apoptotic pathway, thereby inducing apoptosis in H1299 cells.

In summary, in the present study, alkaline protease was selected to enzymatically hydrolyze a Nereid homogenate at 50˚C and pH 10 for 6 h. The material-to-liquid ratio was 1:1 and the amount of enzyme added was 400 U/g. An NOP with a molecular weight of 847 kDa was obtained after separation and purification through ultrafiltration, ion exchange chromatography, gel filtration chromatography, and HPLC. The amino acid sequence of the NOP was Gln-Ile-Asn-Gln-His-Leu. Collectively, the present findings indicated that NOP could inhibit the proliferation of H1299 cells in a dose- and time-dependent manner. Apoptosis in H1299 cells may be triggered by downregulation of Bcl-2 protein, upregulation of Bax protein, and stimulation of the cascade reaction of the caspase family. NOP did not exert a toxic effect on PC12 and SK-N-SH cells; in contrast, it promoted cell proliferation. The limitation of the present study is that the yield of separated and purified samples was relatively low, and it is hoped to improve the yield of samples in the future. In subsequent studies, the precise action pathway and specific action compounds will be further studied.

Acknowledgements

Not applicable.

Funding

This work was supported by the Youth Fund of Zhejiang Academy of Medical Sciences (grant no. C51912Q-04).

Availability of data and materials

The datasets used and/or analyzed during the current study are available from the corresponding author on reasonable request.

Authors' contributions

LS conceived and designed the experiments. GZ, HL, SL, ML and LT performed the experiments and statistical analysis of the data. GZ and HL contributed equally to this study and share first authorship. All authors contributed to the writing of the manuscript and read and approved the final manuscript. LS and GZ confirm the authenticity of all the raw data.

Ethics approval and consent to participate

Not applicable.

Patient consent for publication

Not applicable.

Competing interests

The authors declare that they have no competing interests.

References

1. Guo Q: Current situation of medical treatment of non-small cell lung cancer. Chin J Cancer Prev Treat 16: 721-725, 2009.
2. Ahmed S, Mirzaei H, Aschner M, Khan A, Al-Harrasi A and Khan H: Marine peptides in breast cancer: Therapeutic and mechanistic understanding. Biomed Pharmacother 142: 112038, 2021.
3. Shi F, Yan X, Cheong KL and Liu Y: Extraction, purification, and characterization of polysaccharides from marine algae gracilaria lemaneiformis with anti-tumor activity. Process Biochem 73: 197-203, 2018.
4. Huang ZZ, Du X, Ma CD, Zhang RR, Gong WL and Liu F: Identification of antitumor active constituents in polygonatum sibiricum flower by UPLC-Q-TOF-MS^E and network pharmacology. ACS Omega 5: 29755-29764, 2020.
5. Margolin K, Longmate J, Synold TW, Gandara DR, Weber J, Gonzalez R, Johansen MJ, Newman R, Baratta T and Doroshow JH: Dolastatin-10 in metastatic melanoma: A phase II and pharmokinetic trial of the California cancer consortium. Invest New Drugs 19: 335-340, 2001.

6. Takahashi T, Furukawa Y, Muneoka Y, Matsushima O, Ikeda T, Fujita T, Minakata H and Nomoto K: Isolation and characterization of four novel bioactive peptides from a polychaete annelid, *Perinereis vancaurica*. Comp Biochem Physiol C Pharmacol Toxicol Endocrinol 110: 297-304, 1995.
7. LI Q: Purification, characterization and pharmacodynamic activity of proteases and its isoenzyme from *Nereis virens* (unpublished PhD thesis). Jilin University, 2008.
8. Bai R, Li Q, Liu J, Jiang X and Hong M: Effects of *Nereis virens* proteinase on platelet aggregation and hemorheology. Chin J New Drugs 18: 930-933, 2009 (In Chinese).
9. Bo Q, Ge X, Cui J, Jiang X, Liu J and Hong M: Effects of acidic serine protease ASPNJ on inhibition and injury of leukemia cell K562. Chin J Biochem Pharm 33: 736-739, 2012 (In Chinese).
10. Ge X, Bo Q, Hong X, Cui J, Jiang X, Hong M and Liu J: A novel acidic serine protease, ASPNJ inhibits proliferation, induces apoptosis and enhances chemo-susceptibility of acute promyelocytic leukemia cell. Leuk Res 37: 1697-1703, 2013.
11. McNair K, Forrest CM, Vincenten M, Darlington LG and Stone TW: Serine protease modulation of dependence receptors and EMT protein expression. Cancer Biol Ther 20: 349-367, 2019.
12. Zhang G, Yang M, Ding G, Huang F and Zhao Y: Study on the mechanism of apoptosis induced by SPC-A-1 cells in human lung cancer. Mod Food Technol 31: 6-11, 2015.
13. Yoon SK, Sung SK, Lee DH and Kim HW: Tissue inhibitor of metalloproteinase-1 (TIMP-1) and IL-23 induced by polysaccharide of the black hoof medicinal mushroom, phellinus linteus (Agaricomycetes). Int J Med Mushrooms 19: 213-223, 2017.
14. Pan W, Liu X, Ge F, Han J and Zheng T: Perinerin, a novel antimicrobial peptide purified from the clamworm *Perinereis aibuhitensis* grube and its partial characterization. J Biochem 135: 297-304, 2004.
15. Chen X, Luo Y, Qi B, Luo J and Wan Y: Improving the hydrolysis efficiency of soy sauce residue using ultrasonic probe-assisted enzymolysis technology. Ultrason Sonochem 35: 351-358, 2017.
16. Jiang Z, Xu Y and Su Y: Preparation process of active enzymolysis polypeptides from seahorse bone meal. Food Sci Nutr 2: 490-499, 2014.
17. Qu W, Ma H, Jia J, He R, Luo L and Pan Z: Enzymolysis kinetics and activities of ACE inhibitory peptides from wheat germ protein prepared with SFP ultrasound-assisted processing. Ultrason Sonochem 19: 1021-1026, 2012.
18. Kitts DD and Weiler K: Bioactive proteins and peptides from food sources. Applications of bioprocesses used in isolation and recovery. Curr Pharm Des 9: 1309-1023, 2003.
19. Qian B, Zhao X, Yang Y and Tian C: Antioxidant and anti-inflammatory peptide fraction from oyster soft tissue by enzymatic hydrolysis. Food Sci Nutr 8: 3947-3956, 2020.
20. Maqsoudlou A, Sadeghi MA, Mora L, Mohebodini H, Ghorbani M and Toldrá F: Controlled enzymatic hydrolysis of pollen protein as promising tool for production of potential bioactive peptides. J Food Biochem 43: e12819, 2019.
21. Zhou J: Fucoidan extraction, purification, structure analysis and antioxidant research (unpublished PhD thesis). Hangzhou: Zhejiang University, 2006.
22. Zhu S, Chen M, Niu Q, Li T, Qu Y and Chen Y: Physico-chemical properties and structure analysis of viscera polysaccharide of urechis unicinctus and its lipid peroxidation inhibition activity. Food Sci 36: 67-71, 2015 (In Chinese).
23. Huang F, Yang Z, Yu D, Wang J, Li R and Ding G: Sepia ink oligopeptide induces apoptosis in prostate cancer cell lines via caspase-3 activation and elevation of Bax/Bcl-2 ratio. Mar Drugs 10: 2153-2165, 2012.
24. Ding G, Huang F, Yang Z, Yu D and Yang Y: Anticancer activity of an oligopeptide isolated from hydrolysates of sepia ink. Chin J Nat Med 9: 151-155, 2011.
25. Grela E, Kozłowska J and Grabowiecka A: Current methodology of MTT assay in bacteria-a review. Acta Histochem 120: 303-311, 2018.
26. Ma Y, Zhou B, Sun X, Zhang L, Song L and Xiao H: The effect of diosone active component on the proliferation of glomerular mesangial cells was determined by MTT assay. Tradit Chin Med Inf 27: 34-36, 2010.
27. Chen M, Ge A, Cui P and Liao Z: Study on inhibition effects of phycoerythrin from *Gracilaria lemaneiformis* on Hela cells and its mechanism. Food Sci 28: 549-552, 2007 (In Chinese).
28. Pettit GR, Kamano Y, Herald CL, Tuinman AA, Boettner FE, Kizu H, Schmidt JM, Baczynskyj L, Tomer KB and Bontems RJ: The isolation and structure of a remarkable marine animal antineoplastic constituent: Dolastatin 10. J Am Chem Soc 109: 6883-6885, 1987.
29. Cao W and Song J: Progress in the antitumor polypeptide Aplysia toxin 10 and its derivatives of marine organisms. Grad Med J 24: 1208-1211, 2011 (In Chinese).
30. Shnyder SD, Cooper PA, Millington NJ, Pettit GR and Bibby MC: Auristatin PYE, a novel synthetic derivative of dolastatin 10, is highly effective in human colon tumour models. Int J Oncol 31: 353-360, 2007.
31. Chi CF, Hu FY, Wang B, Li T and Ding GF: Antioxidant and anticancer peptides from the protein hydrolysate of blood clam (Tegillarcagranosa) muscle. J Funct Foods 15: 301-313, 2015.
32. Yao R Chu X, Chen S, Wang C and Liu W: Experimental study on the antitumor effects of polypeptides. Chin Pharm J 41: 868-870, 2006.
33. Wang C, Liu M, Wang F and Lin X: Growth-inhibition effects of a novel anti-tumor polypeptide from *Meretrix meretrix* Linnaeus associated with tubulin polymerization. Chin J Biochem Pharm 33: 225-228, 2012 (In Chinese).
34. Zhu X: Progress in studying the morphological characteristics and molecular mechanisms of cell apoptosis. Chin J Gerontol 31: 2595-2597, 2011 (In Chinese).
35. Chio S, Lew KL, Xiao H, Herman-Antosiewicz A, Xiao D, Brown CK and Singh SV: D,L-Sulforaphane-induced cell death in human prostate cancer cells is regulated by inhibitor of apoptosis family proteins and Apaf-1. Carcinogenesis 28: 151-162, 2007.
36. Clark CS and Maurelli AT: Shigella flexneri inhibits staurosporine-induced apoptosis in epithelial cells. Infect Immun 75: 2531-2539, 2007.
37. Chen ZQ, Jie X and Mo ZN: Curcumin inhibits growth, induces G1 arrest and apoptosis on human prostatic stromal cells by regulating Bcl-2/Bax. Zhongguo Zhong Yao Za Zhi 33: 2022-2025, 2008 (In Chinese).
38. Liu W, Hμang XF, Qi Q, Dai QS, Yang L, Nie FF, Lu N, Gong DD, Kong LY and Guo QL: Asparanin A induces G(2)/M cell cycle arrest and apoptosis in human hepatocellular carcinoma HepG2 cells. Biochem Biophys Res Commun 381: 700-705, 2009.
39. Xu X, Liu Y, Wang L, He J, Zhang H, Chen X, Li Y, Yang J and Tao J: Gambogic acid induces apoptosis by regulating the expression of Bax and Bcl-2 and enhancing caspase-3 activity in human malignant melanoma A375 cells. Int J Dermatol 48: 186-192, 2009.
40. Bhattacharjee M, Acharya S, Ghosh A, Sarkar P, Chatterjee S, Kumar P and Chaudhuri S: Bax and Bid act in synergy to bring about T11TS-mediated glioma apoptosis via the release of mitochondrial cytochrome c and subsequent caspase activation. Int Immunol 20: 1489-1505, 2008.
41. Liu HR, Peng XD, He HB, Wang YH, Li Y, He GX, Liu YL, Li YL and Zeng CJ: Antiproliferative activity of the total saponin of solanum lyratum thunb in Hela cells by inducing apoptosis. Pharmazie 63: 836-842, 2008.
42. Bressenot A, Marchal S, Bezdetnaya L, Garrier J, Guillemin F and Plénat F: Assessment of apoptosis by immunohistochemistry to active caspase-3, active caspase-7, or cleaved PARP in monolayer cells and spheroid and subcutaneous xenografts of human carcinoma. J Histochem Cytochem 57: 289-300, 2009.